

InGaAs nBn SWIR detector design with lattice-matched InAlGaAs barrier

Fatih UZGUR¹, Serdar KOCAMAN^{1,2*}

¹Department of Micro- and Nanotechnology, Graduate School of Natural and Applied Sciences, Middle East Technical University, Ankara, Turkey

²Department of Electrical and Electronics Engineering, Faculty of Engineering, Middle East Technical University, Ankara, Turkey

Received: 26.02.2018

Accepted/Published Online: 23.07.2018

Final Version: 22.01.2019

Abstract: Dark current optimization with band gap engineering has been numerically studied for InGaAs nBn type infrared photodetectors. Undoped InAlGaAs grading layers are utilized in constructing the barrier and dipole delta-doped layers are placed in both sides of the graded layers for eliminating valence band offset. As a result, the high band gap barrier layer blocks the majority carriers and allows minority carrier flow while minimizing various dark current components, as expected from an nBn detector. Substantial improvement has been shown in the dark current level without compromising any photoresponse compared to the conventional pn junction and recently proposed all InGaAs nBn type photodetectors.

Key words: Infrared imaging, barrier photodetectors, optoelectronic devices

1. Introduction

The short wave infrared (SWIR) region (from 0.9 μm to 1.7 μm wavelength range) is quite important for both commercial and military sensing technologies with applications in science, medicine, space exploration, and security. InGaAs with a lattice-matched configuration to InP produces low enough dark current at room temperature, which makes it the most convenient choice for many applications [1–3]. Out of two main detector pixel types, planar structured devices have lower dark current due to the buried absorber layer, and mesa structured devices also have some advantages such as wider application alternatives including dual/multicolor implementation and lower crosstalk due to the isolated pixels [4, 5].

In order to optimize the dark current performance, many methods including post pixel processing passivation and various epilayer designs have been developed, but none of these techniques have fully eliminated the leakage at the surface [6–12]. Relatively recently, barrier structured detectors have been numerically and experimentally shown to produce lower dark current than conventional pn junction detectors and to operate at higher operation temperatures [13–35]. In nBn type barrier detectors, Fermi level between all of the layers are aligned by design while the energy barrier only exists for the majority carriers. Therefore, there is almost no depletion region ideally and various dark current mechanisms are suppressed without affecting the photogenerated carriers [16, 21, 24, 29]. For a successful design, the most critical point is preventing a valence band offset that could block minority carriers as well. To be able to achieve this, various techniques such as simultaneous grading of composition and doping concentration, p-type doped barriers, superlattice

*Correspondence: skocaman@metu.edu.tr

based designs, and use of delta-doping layers have been applied both numerically and experimentally [30–34]. Regarding the InGaAs based SWIR detectors, both pn with barrier and nBn type detectors have been shown to provide successful results [13, 33, 34], and here a novel nBn detector with lower dark current is numerically proposed. The barrier layer (together with the delta-doped layers similar to all InGaAs designs [33]) is designed with an InAlGaAs quaternary compound that linearly grades from low band gap to high band gap by changing the ratio of the Al-Ga mole fraction so that the lattice-mismatch is minimized. From an experimental point of view, growing quaternary compounds is a challenge, but due to the lattice-match between the barrier and the other layers, there is no need for long grading layers, which are also not ideal [33, 34].

2. Method

Numerical simulations were performed using the Sentaurus TCAD [36], where the designed devices are compared to the conventional pn heterojunction and the recently proposed all InGaAs nBn structure [33] at room temperature (300 K). The InGaAs absorber and InAlAs barrier layers, which are connected through the Al-Ga mole fraction ratio grading of the InAlGaAs layers, are almost lattice-matched to the InP substrate. In Figure 1, representative band diagrams for the epilayer structures of the proposed detector type together with the well-known device structures are shown. The conventional pn structure (Figure 1a) suffers from surface leakage current, making passivation one of the most important points [12]. Various barrier designs (Figures 1b and 1c) block some dark current components but still have the depletion region, leading to partially optimized structures [22]. The proposed structure here (Figure 1d) aims to provide a novel nBn design that has both advantages and disadvantages compared to the recently proposed structure [33]. In other words, the purpose here is to introduce an alternative approach that can be useful depending on the fabrication capabilities. In terms of the dark current components, Auger, SRH, and surface recombination mechanisms are considered in the same way as with the all InGaAs design [33].

In compositional gradable materials, quasioelectric fields emerge due to the grading of the band gap. Since the energy band gap becomes composition (position)-dependent, conduction and valence bands' slopes may not be equal; therefore, electrons and holes may be affected by different electric fields, especially depending on the doping [37]. In Figure 2, E_c and E_v are conduction and valence band edges, respectively, whereas F_e and F_h are “quasioelectric” fields resulting from the slope of conduction and valence bands. Figure 2a represents the

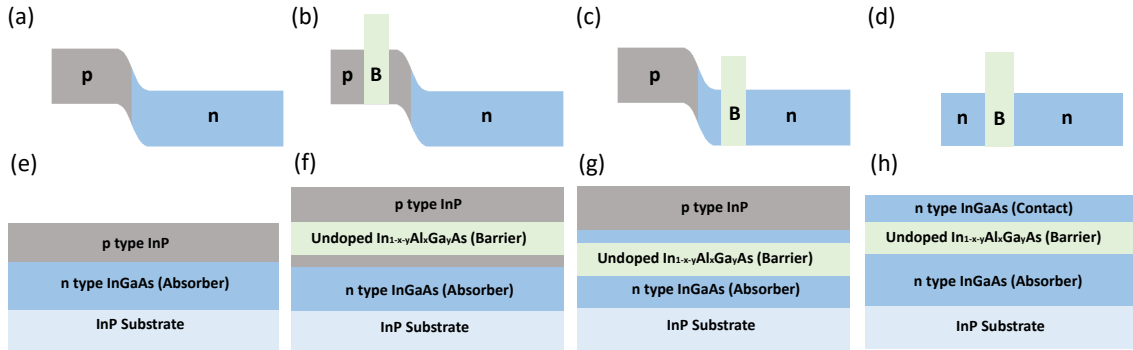


Figure 1. (a-d) Schematic representation for InGaAs/InP heterojunction design and various barrier alternatives. (e-h) Epilayer structures for the schematics in (a-d). As there is almost no depletion region and a barrier for the surface leakage, dark current is expected to be low in the nBn structure in (d).

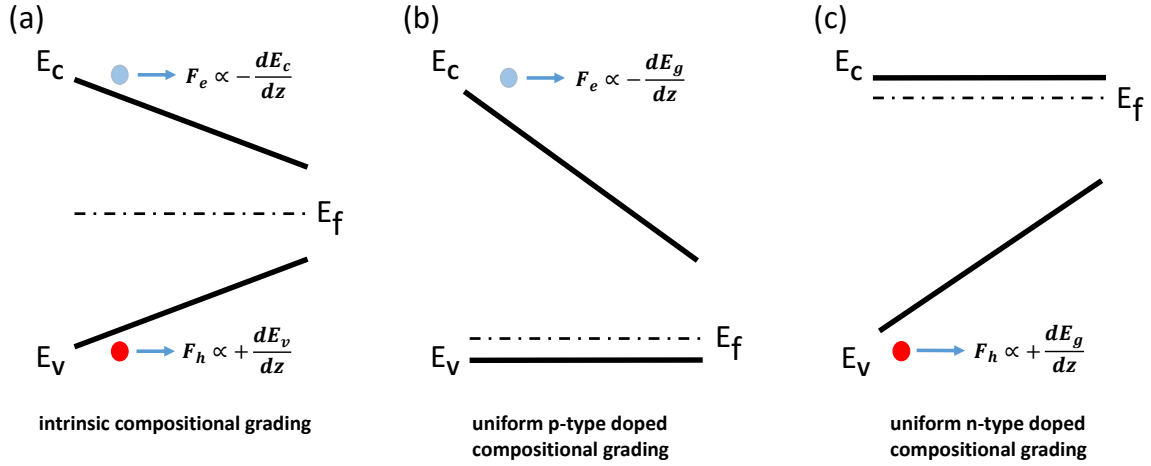


Figure 2. Band diagrams of compositional graded compound; (a) undoped, (b) p-type doped, and (c) n-type doped.

case where there is an undoped graded compound. In this configuration, electrons and holes move in the same direction under F_e and F_h quasidelectric fields.

Furthermore, in Figure 2b, a band structure for a uniform p-type doped graded compound is shown, and due to the flat valence band, there is no “quasidelectric” field on the holes and electrons feel more force compared to the undoped case coming from the band offset transferred to the conduction band. In Figure 2c, the same effect is illustrated for the uniformly n-type doped graded compound [38]. As shown in Figures 2b and 2c, barrier structures can actually be built by only using uniformly doped graded material. However, these barrier structures will block minority carriers and allow majority carriers since their doping is the same as the absorber and this behavior is the opposite of the expected functionality from an ideal detector structure with barrier[24]. In order to achieve the useful barrier case, the doping type should be changed, but that would effectively lead to a pn junction with depletion region and the dark current mechanisms would not be satisfactorily eliminated. Therefore, additional band diagram engineering methods are necessary for the desired characteristics.

In this work, in order to construct a high band gap barrier layer, $\text{In}_{1-x-y}\text{Al}_x\text{Ga}_y\text{As}$ quaternary compound graded from InGaAs to InAlAs is utilized while maintaining $x+y=0.47$ to preserve the lattice constant [39]. Figure 3a represents the band diagram of this structure with no additional adjustment where there are both conduction and valence band barriers leading to a minority barrier in addition to the desired majority carrier barrier.

In order to fix the minority carrier barrier, n-type and p-type delta-doped layers are placed at the sides of the graded layers. Consequently, the valence band quasidelectric field has been canceled and the valence band offset is suppressed, resulting in an almost ideal nBn detector profile as shown in Figure 3b. This methodology is actually the same as that for the recently proposed all InGaAs structure [33]. However, as illustrated in Figure 4, having lattice-matched layers will result in a better quality material with a shorter material growth time by removing the need for relatively longer grading layers that are necessary to minimize the effects from lattice-mismatch.

As shown in Figures 4a and 4b, the regular pn junction has a depletion region and various dark current mechanisms are maximized at the depletion region. Figures 4c and 4d represents the all InGaAs nBn structure where relatively thicker grading structures are required due to the lattice-mismatch coming from the InGaAs compositional grading. However, a similar barrier structure can be achieved without introducing lattice-

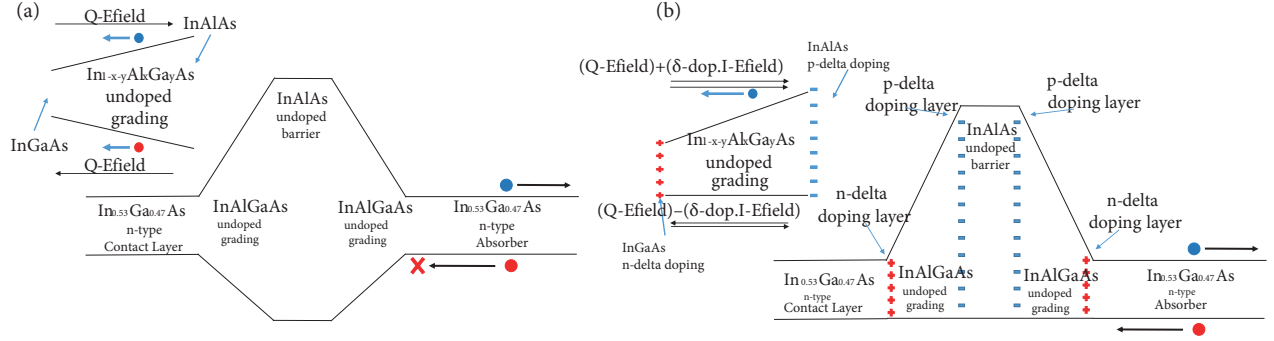


Figure 3. Schematic band diagram of valence band for (a) uncompensated and (b) adjusted with delta-doped layers InGaAs nBn detector.

mismatch in the case of InAlAs barrier layer and InAlGaAs grading layers, as seen in Figures 4e and 4f. As the benefit here comes from quaternary compounds (more difficult material growth), the idea here is to present a novel structure that could be useful in the case that modern sophisticated material growth capabilities are available.

Reverse biased band diagram characteristics for the structures shown in Figure 4 are presented in Figure 5, where Figure 5a shows the pn junction ($N_d = 5 \times 10^{16} \text{ cm}^{-3}$, $N_a = 5 \times 10^{16} \text{ cm}^{-3}$) and Figures 5b and 5c illustrate the nBn structures discussed above. The nBn designs both include an InGaAs lattice-matched absorber ($N_d = 5 \times 10^{16} \text{ cm}^{-3}$), contact layer ($N_d = 6 \times 10^{16} \text{ cm}^{-3}$), high bandgap barrier (undoped), and linearly compositional graded (undoped) and dipole delta-doped ($N_d = N_a = 1.1 \times 10^{18} \text{ cm}^{-3}$) layers where the valence band offset is removed with the help of delta-dopings [13, 33, 34, 40, 41]. Doping levels are chosen considering the case where absorber doping up to low 10^{17} cm^{-3} levels has been shown to lower the dark current [42].

3. Results

Next, dark and photocurrent calculations including sensitivity analysis with respect to different delta-doping concentrations and various barrier heights adjusted by Al-Ga mole fraction ratio are discussed for the proposed nBn detector. In the simulations, optical calculations were done at $1.55 \mu\text{m}$ under 0.01 W/cm^2 optical power per unit area in the normal direction to the epitaxial structure from the substrate side (back illuminated) while the absorption coefficient of $\text{In}_{0.53}\text{Ga}_{0.47}\text{As}$ at $1.55 \mu\text{m}$ was considered as 7000 cm^{-1} [13, 33, 43].

Figure 6a shows the dark and photocurrent densities versus delta-doping layer concentrations and Figure 6b illustrates the adjustable valence and conduction band offsets with delta-doping layer doping concentrations. At the lower delta-doping concentrations, the valence band barrier blocks the minority carriers; therefore, the detector exhibits lower photocurrent and the dark current is higher since the thermionic emission can flow over the barrier to the absorber. When the doping concentrations are increased, the flow of minority carrier is getting easier (photocurrent density increases) due to lowered valence band offset. Simultaneously, the dark current density decreases because of more efficient blocking of the majority carriers (Figure 6b). When delta-doping concentrations are increased to $1.1 \times 10^{18} \text{ cm}^{-3}$, valence band offset is almost completely eliminated

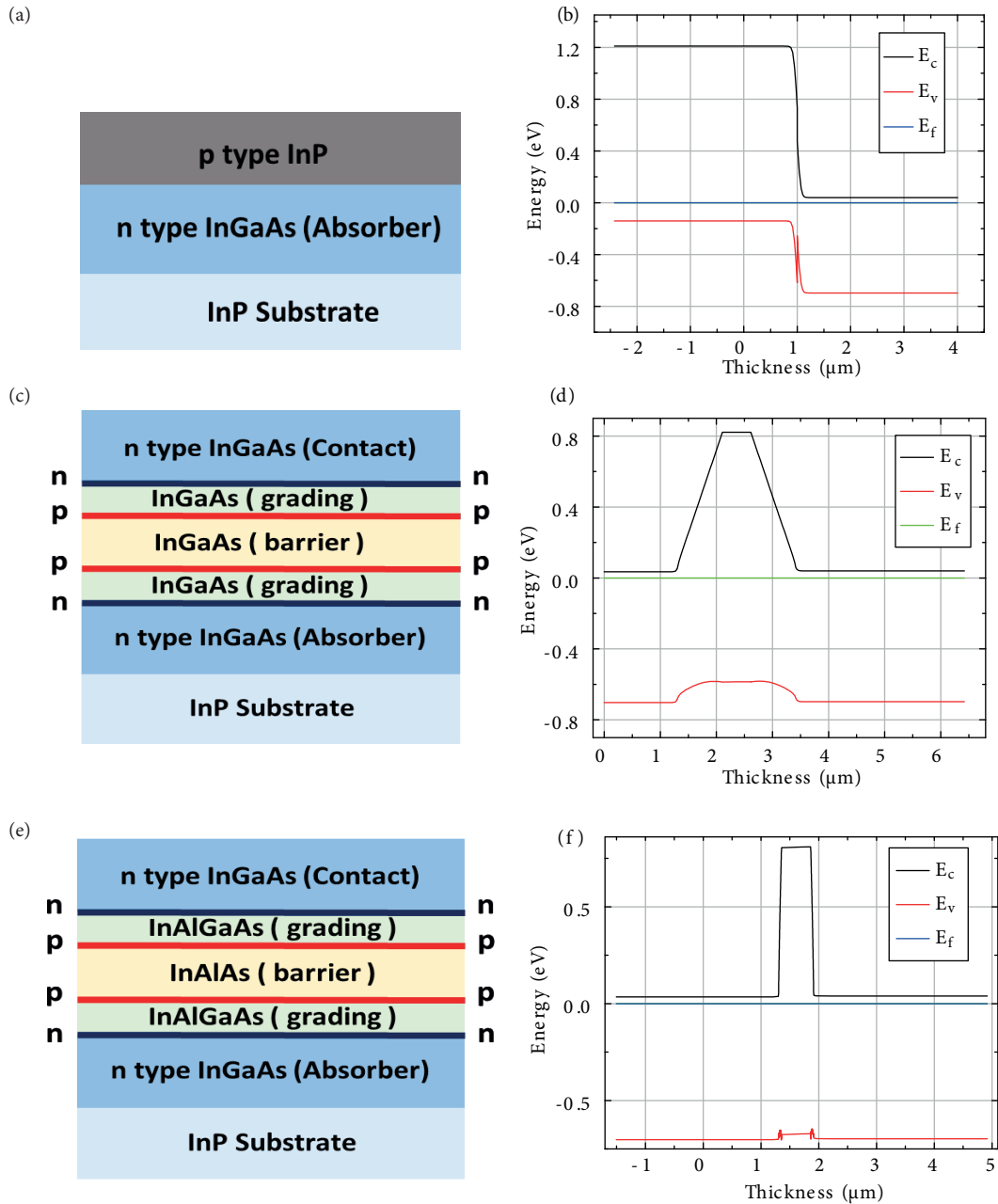


Figure 4. Pixel structure and calculated band diagram for (a, b) a pn junction, (c, d) nBn detector with all InGaAs epilayers [33], and (e, f) nBn detectors with all lattice-matched epilayers (structure proposed here). Absorber layers are 3 μm for all cases. Barrier layers are 500 nm and delta-dopings are 5 nm for both nBn structures. Grading layer is around 800 nm for the lattice-mismatched case and 50 nm for the lattice-matched case.

and conduction band offset becomes high enough to block majority carrier electrons effectively, leading to the optimum nBn performance characteristics. Furthermore, if the delta-doping concentrations are increased even more, the high electric field causes higher thermal SRH generation and increases the dark current (Figure 6a).

Figure 7a shows effects of the barrier height coming from the Al-Ga mole fraction ratio change on the dark and photocurrent density characteristics of the designed nBn detectors. Here, the barrier layer is constructed by

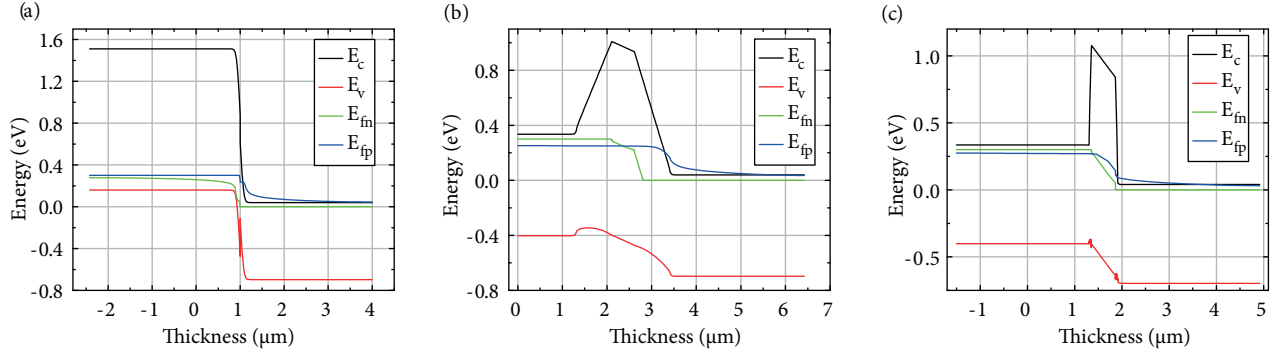


Figure 5. Reverse biased band diagrams for the structures shown in Figure 4 with a reverse bias of 0.3 V: (a) pn heterojunction, (b) all InGaAs nBn structure, (c) lattice-matched nBn structure.

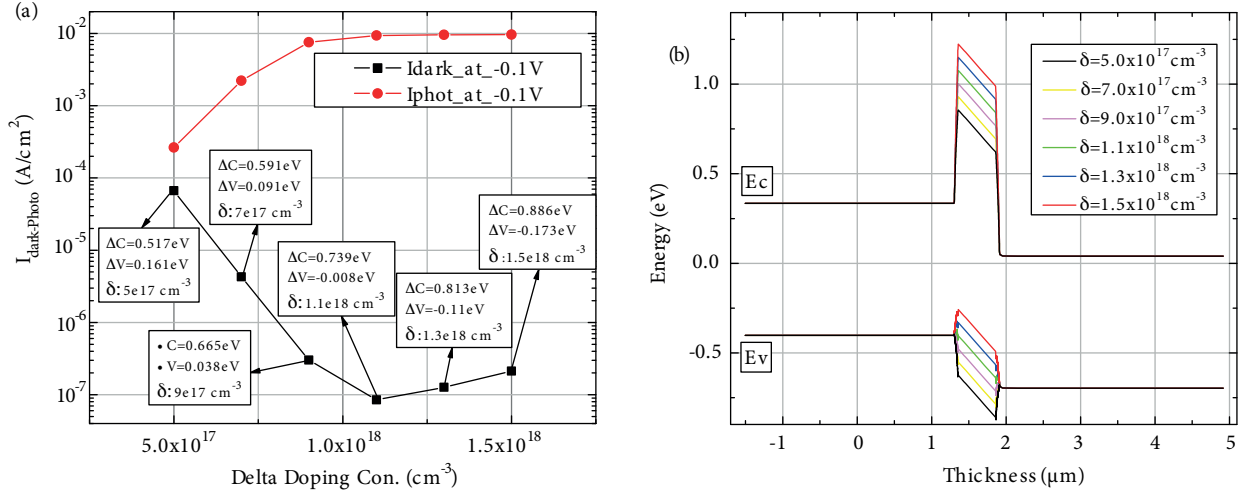


Figure 6. Effects of different delta-doping layer doping concentration on (a) photocurrent and dark current densities and (b) band diagram of the nBn detector.

compositional grading of InAlGaAs material from InGaAs to various Al-Ga ratios together with the optimized delta-doping concentrations, providing zero valence band offset for each barrier height (Figure 7b). At the lower barrier heights (low Al-Ga ratios), majority carriers can overcome the barrier by thermionic emission, so that the dark current becomes higher and photocurrent is suppressed by the high dark current. When the Al-Ga ratio of the barrier increases, the barrier height increases and the majority carriers are consequently blocked, resulting in a reduced dark current density.

Moreover, in order to visualize the relative performance of the proposed nBn structure, total dark and photocurrent densities of the two nBn designs and the pn heterojunctions are comparatively analyzed. Results are summarized in Figure 8, where Figure 8a shows the dark current density comparison and the photoresponse characteristics are seen in Figures 8b and 8c. The band gap engineered lattice-matched InGaAs nBn detector clearly and conclusively exhibits lower dark current without photocurrent degradation, as expected from an ideal nBn detector. Calculated dark current density for the conventional pn heterojunction is similar to the recently reported experimental values for the mesa type detectors [4]. As a result, around 50 and 2.5 times improvement has been shown in the dark current density level compared to the conventional pn junction and

recently proposed all InGaAs nBn type photodetector, respectively.

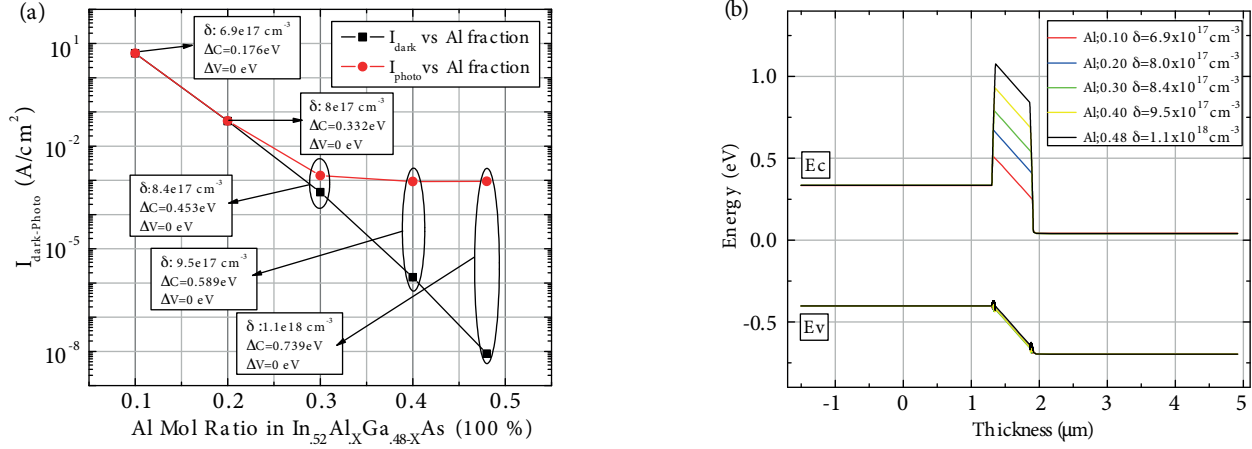


Figure 7. Effects of different barrier heights with optimized delta-doping concentrations on (a) photocurrent and dark current densities and (b) band diagram of the nBn detector. ΔV (ΔC) represents the valence (conduction) band offsets.

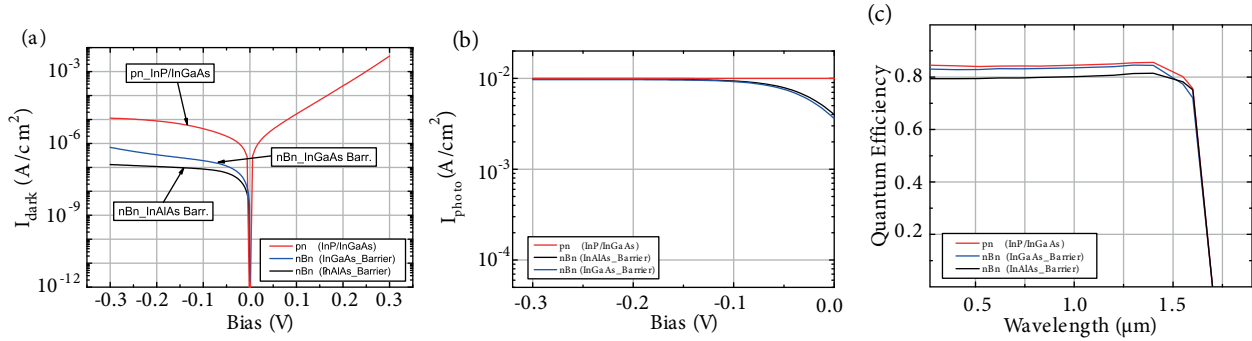


Figure 8. Dark and photocurrent density results together with the quantum efficiency values at -0.2 V of the proposed InGaAs nBn in comparison with conventional InGaAs pn heterojunction detector and recently proposed nBn structure.

The same carrier lifetime and surface recombination velocity values have been used for all structures in the comparison in Figure 8 and the calculated dark current density for the proposed structure is getting closer to the record values reported for planar type detectors [44, 45]. Considering the effects of lattice-mismatch on the carrier lifetime, the improvement for the all lattice-matched case compared to the lattice-mismatched case would be even stronger.

4. Conclusion

In summary, a novel InGaAs nBn detector design has been realized by utilizing lattice-matched materials and band gap engineering techniques. The barrier layer that is supposed to block the majority carriers and allow the minority carriers so that the dark current is suppressed without any compromise in photoresponse is obtained by using compositional grading of InAlGaAs and delta-doping layers. Barrier layer thickness and height are design parameters for obtaining zero valence band offset. The proposed structure shows a substantial reduction in dark current compared to the previous designs. Techniques discussed here give a degree of freedom for various detector designs with various material systems.

References

- [1] Bommena R, Bergeson JD, Kodama R, Zhao J, Ketharanathan S, Schaake H, Shih H, Velicu S, Aqariden F, Wijewarnasuriya PS et al. High-performance SWIR HgCdTe FPA development on silicon substrates. In: SPIE 2014 Defense + Security; 5–9 May 2014; Baltimore, MD, USA. Bellingham, WA, USA: SPIE. pp. 907009-1–907009-12.
- [2] Nakajima K, Yamaguchi A, Akita K, Kotani T. Composition dependence of the band gaps of In_{1-x}Ga_xAs_{1-y}Py quaternary solids lattice-matched on InP substrates. *J Appl Phys* 1978; 49: 5944-5950.
- [3] Onat BM, Huang W, Masaun N, Lange M, Ettenberg MH, Dries C. Ultra-low dark current InGaAs technology for focal plane arrays for low-light level visible-shortwave infrared imaging. In: SPIE 2007 Defense and Security Symposium; 9–13 April 2007; Orlando, FL, USA. Bellingham, WA, USA: SPIE. pp. 65420L-1–65420L-9.
- [4] Rutz F, Kleinow P, Aidam R, Bronner W, Kirste L, Walther M. InGaAs infrared detector development for SWIR imaging applications. In: SPIE 2013 Security + Defence; 23–26 September 2013; Dresden, Germany. Bellingham, WA, USA: SPIE. pp. 88960C-1-88960C-7.
- [5] Stocker HJ, Aspnes DE. Surface chemical reactions on In_{0.53}Ga_{0.47}As. *Appl Phys Lett* 1983; 42: 85-87.
- [6] Yeats R, Von Dessonneck K. Polyimide passivation of In_{0.53}Ga_{0.47}As, InP, and InGaAsP/InP p-n junction structures. *Appl Phys Lett* 1984; 44: 145-147.
- [7] Ohnaka K, Kubo M, Shibata J. A low dark current InGaAs/InP pin photodiode with covered mesa structure. *IEEE T Electron Dev* 1987; 34: 199-204.
- [8] Kim HS, Choi JH, Bang HM, Jee Y, Yun SW, Burm J, Kim MD, Choo AG. Dark current reduction in APD with BCB passivation. *Electron Lett* 2001; 37: 455-457.
- [9] Yamabi R, Tsuji Y, Hiratsuka K, Yano H. Fabrication of mesa-type InGaAs pin PDs with InP passivation structure on 4-inch diameter InP substrate. In: IEEE 2004 Indium Phosphide and Related Materials Conference; 31 May–4 June 2004; Kagoshima, Japan. New York, NY, USA: IEEE. pp. 245-248.
- [10] Kim O, Dutt B, McCoy R, Zuber, J. A low dark-current, planar InGaAs pin photodiode with a quaternary InGaAsP cap layer. *IEEE J Quantum Electron* 1985; 21: 138-143.
- [11] Tennant WE, Lee DL, Piquette EC. Fully Depleted Diode Passivation Active Passivation Architecture. Google Patents, 2014.
- [12] Dolas MH, Kocaman S. Fully depleted InP nano-layer for in-device passivation of InGaAs SWIR detectors. *IEEE Electron Device Lett* 2017; 38: 1692-1695.
- [13] Klem JF, Kim JK, Cich MJ, Keeler GA, Hawkins SD, Fortune TR. Mesa-isolated InGaAs photodetectors with low dark current. *Appl Phys Lett* 2009; 95: 031112.
- [14] White AM. Infra Red Detectors. Google Patents, 1987.
- [15] Klipstein P. Depletion-less Photodiode with Suppressed Dark Current and Method for Producing the Same. Google Patents, 2010.
- [16] Maimon S, Wicks GW. nBn detector, an infrared detector with reduced dark current and higher operating temperature. *Appl Phys Lett* 2006; 89: 151109.
- [17] Khoshakhlagh A, Rodriguez JB, Plis E, Bishop GD, Sharma YD, Kim HS, Dawson LR, Krishna S. Bias dependent dual band response from In As/ Ga (In) Sb type II strain layer superlattice detectors. *Appl Phys Lett* 2007; 91: 263504–263506.
- [18] Klipstein P. “XBn” barrier photodetectors for high sensitivity and high operating temperature infrared sensors. In: SPIE 2008 Defense and Security Symposium; 16–20 March 2008; Orlando, FL, USA. Bellingham, WA, USA: SPIE. pp. 69402U-1–69402U-12.
- [19] Ting DZY, Hill CJ, Soibel A, Keo SA, Mumolo JM, Nguyen J, Gunapala SD. A high-performance long wavelength superlattice complementary barrier infrared detector. *Appl Phys Lett* 2009; 95: 023508.
- [20] Maimon S. Reduced Dark Current Photodetector. Google Patents, 2010.

- [21] Savich GR, Pedrazzani JR, Sidor DE, Maimon S, Wicks GW. Dark current filtering in unipolar barrier infrared detectors. *Appl Phys Lett* 2011; 99: 121112.
- [22] Savich GR, Pedrazzani JR, Sidor DE, Maimon S, Wicks GW. Use of unipolar barriers to block dark currents in infrared detectors. In: *SPIE 2011 Defense, Security and Sensing*; 25–29 April 2011; Orlando, FL, USA. Bellingham, WA, USA: SPIE. pp. 80122T-1–80122T-10.
- [23] Schuster J, Keasler CA, Reine M, Bellotti E. Numerical simulation of InAs nBn back-illuminated detectors. *J Electron Mater* 2012; 41: 2981-2991.
- [24] Savich GR, Pedrazzani JR, Sidor DE, Wicks GW. Benefits and limitations of unipolar barriers in infrared photodetectors. *Infr Phys Technol* 2013; 59: 152-155.
- [25] Reine M, Schuster J, Pinkie B, Bellotti E. Numerical simulation and analytical modeling of InAs nBn infrared detectors with p-type barriers. *J Electron Mater* 2013; 42: 3015-3033.
- [26] Reine M, Pinkie B, Schuster J, Bellotti E. Numerical simulation and analytical modeling of InAs nBn infrared detectors with n-type barrier layers. *J Electron Mater* 2014; 43: 2915-2934.
- [27] Martyniuk P, Gawron W, Rogalski A. Theoretical modeling of HOT HgCdTe barrier detectors for the mid-wave infrared range. *J Electron Mater* 2013; 42: 3309-3319.
- [28] Martyniuk P, Rogalski A. Theoretical modeling of InAsSb/AlAsSb barrier detectors for higher-operation-temperature conditions. *Opt Eng* 2014; 53: 017106.
- [29] Sidor DE, Savich GR, Du X, Wicks GW. Flat-band pn-based unipolar barrier photodetector. *Infrared Phys Technol* 2015; 70: 111-114.
- [30] Akhavan ND, Umana-Membreno GA, Jolley G, Antoszewski J, Faraone L. A method of removing the valence band discontinuity in HgCdTe-based nBn detectors. *Appl Phys Lett* 2014; 105: 121110.
- [31] Kopytko M, Wróbel J, Józwiowski K, Rogalski A, Antoszewski J, Akhavan ND, Umana-Membreno GA, Faraone L, Becker CR. Engineering the bandgap of unipolar HgCdTe-based nBn infrared photodetectors. *J Electron Mater* 2015; 44: 158-166.
- [32] Akhavan ND, Umana-Membreno GA, Gu R, Asadnia M, Antoszewski J, Faraone L. Superlattice barrier HgCdTe nBn infrared photodetectors: Validation of the effective mass approximation. *IEEE T Electron Dev* 2016; 63: 4811-4818.
- [33] Uzgur F, Karaca U, Kızılkın E, Kocaman S. All InGaAs unipolar barrier infrared detectors. *IEEE T Electron Dev* 2018; 65: 1397-1403.
- [34] Uzgur F, Karaca U, Kızılkın E, Kocaman S. Al/Sb free InGaAs unipolar barrier infrared detectors. *SPIE 2017 Defense+ Security*; 9–13 April 2017; Anaheim, CA, USA. Bellingham, WA, USA: SPIE. pp. 1017706-1–1017706-7.
- [35] Scott JW, Jones CE, Caine EJ, Cockrum CA. Sub-pixel nBn Detector. Google Patents, 2011.
- [36] Synopsys Inc. *Sentaurus Device User Guide*. Version K-2015.06. Mountain View, CA, USA: Synopsys, 2016.
- [37] Kroemer H. Quasi-electric fields and band offsets: Teaching electrons new tricks (Nobel lecture). *ChemPhysChem* 2001; 2: 490-499.
- [38] Capasso F. Compositionally graded semiconductors and their device applications. *Ann Rev Mater Sci* 1986; 16: 263-291.
- [39] Olego D, Chang TY, Silberg E, Caridi EA, Pinczuk A. Compositional dependence of band-gap energy and conduction-band effective mass of $\text{In}_{1-x-y}\text{Ga}_x\text{As}_y$ lattice matched to InP. *Appl Phys Lett* 1982; 41: 476-478.
- [40] Nguyen C, Liu T, Chen M, Sun HC, Rensch D. AllInAs/GaInAs/InP double heterojunction bipolar transistor with a novel base-collector design for power applications. *IEEE Electron Device Lett* 1996; 17: 133-135.
- [41] Capasso F. Band-gap engineering: from physics and materials to new semiconductor devices. *Science* 1987; 235: 172-176.

- [42] Wang XD, Hu WD, Chen XS, Lu W, Tang HJ, Li T, Gong HM. Dark current simulation of InP/InGaAs/InP pin photodiode. In: NUSOD 2008 Numerical Simulation of Optoelectronic Devices; 1–5 September 2008; Nottingham, UK. New York, NY, USA: IEEE. pp.31-32.
- [43] Rogalski A. Infrared Detectors. Boca Raton, FL, USA: CRC Press, 2010.
- [44] Yuan H, Meixell M, Zhang J, Bey P, Kimchi J, Kilmer LC. Low dark current small pixel large format InGaAs 2D photodetector array development at Teledyne Judson Technologies. In: SPIE 2012 Defense, Security and Sensing; 23–27 April 2012; Baltimore, MD, USA. Bellingham, WA, USA: SPIE. pp. 835309-1-835309-8.
- [45] MacDougal M, Geske J, Wang C, Follman D. Low-light-level InGaAs focal plane arrays with and without illumination. In: SPIE 2010 Defense, Security and Sensing; 5–9 April 2010; Orlando, FL, USA. Bellingham, WA, USA: SPIE. pp. 76600K-1-76600K-8.